ELSEVIER

Biochimica et Biophysica Acta 1564 (2002) 165–172

BIOCHIMICA ET BIOPHYSICA ACTA
BBA

www.bba-direct.com

Micromanipulation of phospholipid bilayers by atomic force microscopy

Nobuo Maeda [a,1], Tim J. Senden [a,b,*], Jean-Marc di Meglio [b,2]

[a] *Department of Applied Mathematics, Research School of Physical Sciences and Engineering, The Australian National University, Canberra ACT 0200, Australia*

[b] *Institut Charles Sadron (CNRS UPR 022), 6 rue Boussingault, 67083 Strasbourg Cedex, France*

Received 24 January 2002; received in revised form 27 March 2002; accepted 11 April 2002

Abstract

The molecular details of adhesion mechanics in phospholipid bilayers have been studied using atomic force microscopy (AFM). Under tension fused bilayers of dipalmitoylphosphatidylcholine (DPPC) yield to give non-distance dependent and discrete force plateaux of 45.4, 81.6 and 113 ± 3.5 pN. This behaviour may persist over distances as great as 400 nm and suggests the stable formation of a cylindrical tube which bridges the bilayers on the two surfaces. The stability of this connective structure may have implications for the formation of *pili* and hence for the initial stage of bacterial conjugation. Dimyristoylphosphatidylcholine (DMPC) bilayers also exhibit force plateaux but with a much less pronounced quantization. Bilayers composed of egg PC, sterylamine and cholesterol stressed in a similar way show complex behaviour which can in part be explained using the models demonstrated in the pure lipids.

Keywords: Atomic force microscopy; Vesicle; Tubule; Pilus; Bilayer; Membrane fusion; Phospholipids; SPM

1. Introduction

The process of making liposomes (vesicles) from the swelling of adsorbed multilayer lipids has not yet received a convincing physical interpretation, specially when an external electrical field is applied to form giant unilamellar vesicles (GUV) [1]. More experimental investigation is needed at a mesoscopic scale to elucidate the first stages of water permeation into stacked lipid bilayers. In this paper, we report an investigation of the manipulation of supported phospholipid bilayers in an excess of water with atomic force microscopy (AFM). AFM also provides an alternative and novel way to study the detailed process of phospholipid bilayer *fission*, which has so far received very little attention, on the contrary with the process of membrane *fusion*, which has been studied by using the surface forces apparatus (SFA) [2,3]. AFM constitutes a valuable technique for probing bilayer mechanics on length and energy scales similar to that experienced by colliding cells, and thus might help to understand basic communication and exchange processes between living cells.

2. Materials and methods

All chemicals have been purchased from Sigma-Aldrich and used without any further purification. We have used dipalmitoylphosphatidylcholine (DPPC), dimyristoylphosphatidylcholine (DMPC) and a negative liposome kit (63 μmol of L-α-phosphatidylcholine, 18 μmol of sterylamine and 9 μmol of cholesterol). Fully hydrated DPPC (resp. DMPC) exhibits phase transitions from L_β (the so-called gel state, stiff-chain lamellar phase) to P_β (the ripple phase) and then to L_α (the melted-chain lamellar phase) at 34.4 ± 2.5 °C (resp. 13.7 ± 2 °C) and 41.3 ± 1.8 °C (resp. 23.6 ± 1 °C) [4,5]. Lipid bilayers were prepared by evaporating, in a laminar flow cabinet, 1–3 μl of a 1:1 chloroform/ethanol solution, made of 1 mg of phospholipids in 700 μl, onto freshly cleaved muscovite mica substrates. AFM micrographs of the films under water are shown in Fig. 1. The first aim was to produce films so thick that the surface chemistry of the underlying substrate had little influence

* Corresponding author. Department of Applied Mathematics, Research School of Physical Sciences and Engineering, The Australian National University, Canberra ACT 0200, Australia. Tel.: +61-2-6125-4781; fax: +61-2-6125-0732.

E-mail address: tim.senden@anu.edu.au (T.J. Senden).

[1] Present address: Department of Chemical Engineering and Materials Science, University of California, Santa Barbara CA 93106, USA.

[2] Université Louis Pasteur (Strasbourg I) and Institut Universitaire de France.

0005-2736/02/$ - see front matter
PII: S0005-2736(02)00443-1

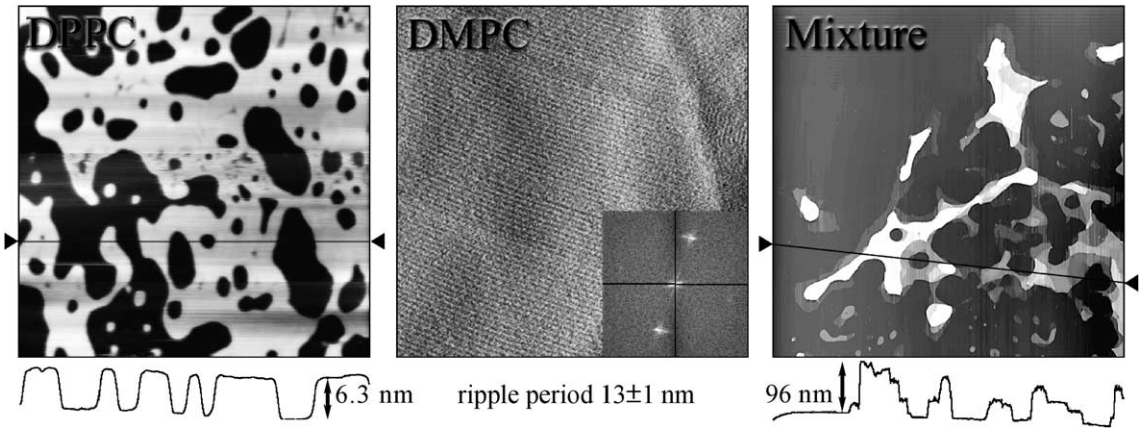

Fig. 1. Typical contact-mode micrographs of thick, multilamellar stacks of DPPC, DMPC and mixture (liposome kit) bilayers in water at room temperature (22 °C). DPPC (image area 4 μm^2): the vertical contrast has been set to emphasize the height difference between the first and second bilayers, 6.3 nm. A cross-section is shown below along a line joining the arrows on the margins of the image. DMPC (image area 1 μm^2): the ripples of the P_β phase are clearly visible; the inset shows the 2D Fourier transform of the image with very well-defined Bragg peaks. Mixture (image area 50 μm^2): hole defects and islands of quantized heights are clearly visible.

over the topmost bilayer; a situation close to the *free* bilayers found in cell membranes [6–8]. In this state, lipid material from the topmost bilayers can be forcibly transferred to the scanning tip, encouraging the formation of symmetric surfaces. In living cells, it is the cytoskeleton which acts to support the membrane. To encourage uniform transfer, the silicon nitride cantilevers (Nanoprobes, Digital Instruments) were rendered hydrophilic by water plasma treatment prior to use.

The lipid-covered mica and treated cantilever were mounted in the commercial fluid cell (Nanoscope III, Digital Instruments) and measurements were carried out in milli-Q water. Prior to force measurements, the cantilever was scanned over an area of several square microns in contact mode to prime the tip with lipid material. The contact force required to initiate this transference was variable and depended on the history of the scanned region, but typically was less than 1 nN. The force measurements were made at speeds ranging from 0.5 to 50 $\mu m \cdot s^{-1}$. Within this range, the measured force profiles showed no speed dependency, suggesting that the measurements were performed in a quasi-static regime avoiding any dissipation-related phenomena. The spring constant of each cantilever was calibrated in situ using a hydrodynamic method [9].

3. Results and discussion

3.1. DPPC bilayers

Experiments were carried out at 22 ± 1 °C, which is well inside the gel state domain. Fusion of opposed DPPC bilayers has been observed (Fig. 2, open symbols) by several groups previously [2,3]. This is characterised by a spring instability, or jump-in, just prior to compliance, in which the cantilever becomes the most compliant component of the system. This condition defines the relative zero of surface separation. The jump-in distance ranges from around the thickness of one lipid molecule to that of a bilayer (Fig. 3). The force at which this jump-in occurs is also variable, and reflects the variability noted when scanning. In general, the magnitude of this force diminishes with the number of compressions performed. This suggests that membrane damage is cumulative, probably exaggerated by the gel-like state of the lipid tails. Unfortunately, the details of the fusion process obtained using the SFA, such as propagation of hemifused section from a high pressure region to low pressure regions [2,3], are not accessible with AFM. However, the details of the fission process, which have been inaccessible in SFA due to the relatively large area of contact, are accessible by AFM. If, on compression, a jump-in does not occur, then the separation force profile is identical to the approach profile. The presence of a jump-in signals that a primary adhesion will occur upon separation and, in around 20 % of cases, a constant force plateau will also be recorded (Fig. 2, filled symbols). This figure shows three examples of plateau events. Profile A is by far the most common, but on occasions two plateaux occur simultaneously, profile B. Very rarely, three plateaux can be observed, profile C. The distance and force where these phenomena no longer bridge the two surfaces, the point of release, are tabulated in Fig. 4. The magnitude of the single plateaux is at 45.4 ± 3.5 pN, with the double and triple events occurring at 81.6 ± 3.5 pN and 113 ± 3.5 pN, respectively (Fig. 5). Unlike the magnitude of the plateaux, the range in distance is not discrete and is roughly exponentially distributed, decreasing in frequency with distance with a decay length $\simeq 95$ nm.

The combination of bilayer fusion and the long-range nature of the plateaux suggest that bilayer fragments are

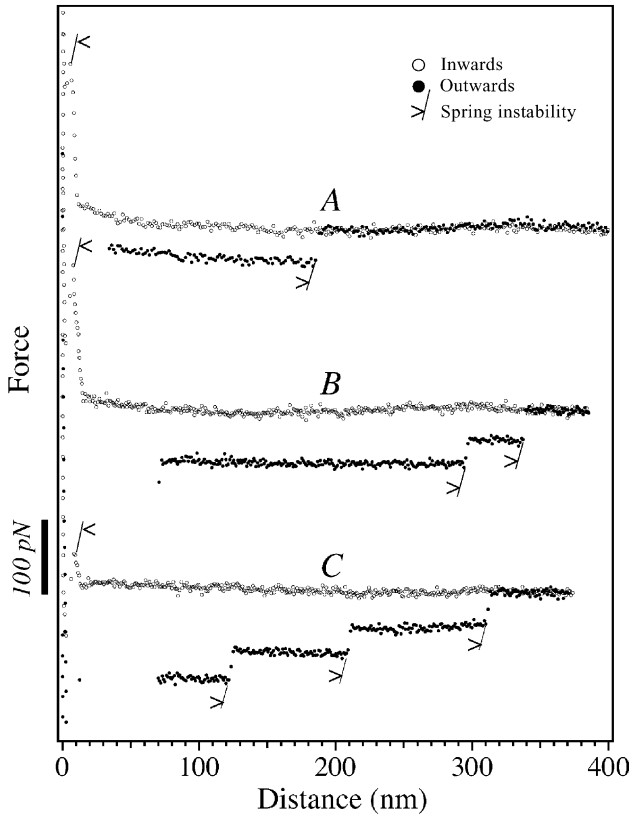

Fig. 2. Three typical force profiles showing plateau events: (A) a common single event, (B) an infrequent double plateau profile, and (C) a rare triple plateau profile. Open symbols show data on approach of the two surfaces, filled symbols on separation.

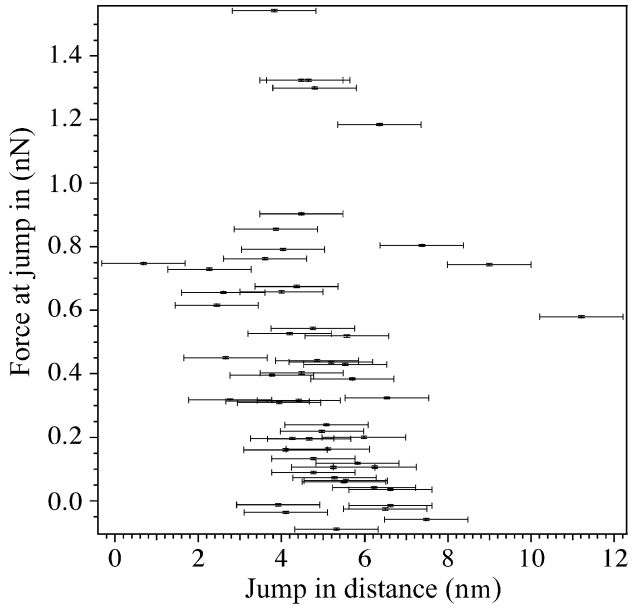

Fig. 3. DPPC: collected statistics for the jump-in distances on approach depicting bilayer fusion resulting from the displacement of between one monolayer to one bilayer (the DPPC bilayer thickness is 4.7 nm and the repeat distance of the fully hydrated L_{β} phase is 6.4 nm [10]). Error bars: distance $\pm$ 1 nm, force $\pm$ 3.5 pN. The error in the force is represented by the rms noise in the baseline.

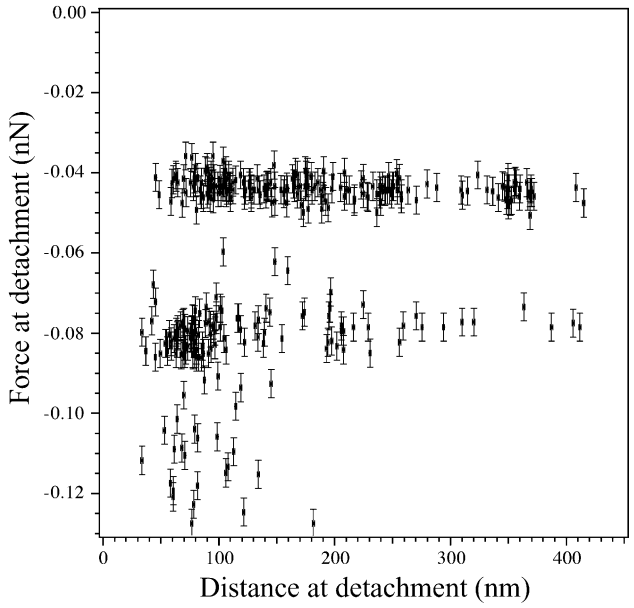

Fig. 4. DPPC: a scatter plot showing the points of plateau release for the data binned in Fig. 5. Error bars: distance $\pm$ 1 nm, force $\pm$ 3.5 pN.

being extended between the two surfaces. The absence of any elastic or restoring forces in this process indicates two main features. Firstly, the fused bilayer fragments slide over each other in the aqueous layer which separates them. The relatively high energetic cost of exposing the hydrophobic inner membrane precludes the sliding of the tails over each other. The second feature relates to the geometry of the fragment. Extending an arbitrarily shaped strip would introduce a distance dependency in the profile simply due to the

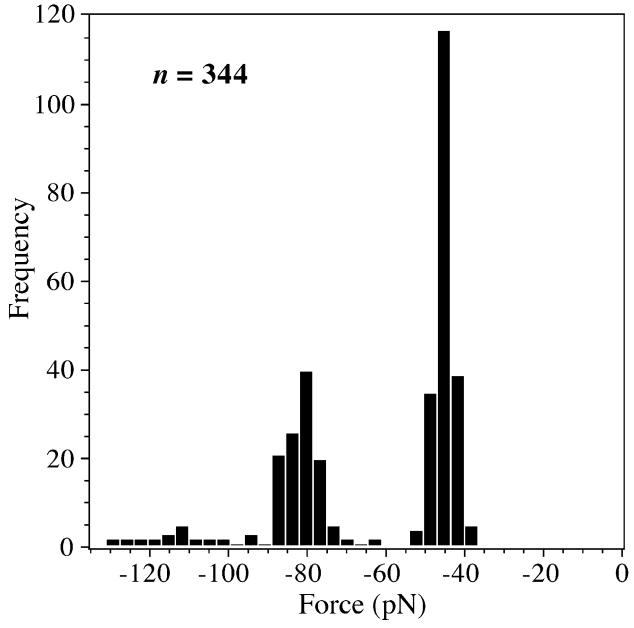

Fig. 5. DPPC: a histogram showing discrete nature of the plateau events (344 events). The distribution peaks at 45.4, 81.6 and 113 $\pm$ 3.5 pN.

changing width of the fragment. The repeated symmetric extension of uniform strips over several hundred nanometres long is highly improbable, giving the low degree of lateral order within the gel-like bilayers. A plausible alternative is formation of a uniform vesicular tube of discrete radius. It is known that giant vesicles under an external shear flow deform into a tubular structure (tether) above the chain melting temperature of the lipids [11–18]. The bending modulus, κ, for a simple thin-walled cylinder can be expressed in terms of radius, r and the tensile force, F as;

$$\kappa = Fr/\pi \tag{1}$$

The force profiles which exhibit multiple plateaux suggest the extension of concentric tubes, and are not simply a consequence of independent tubes. This follows from the magnitudes of the second and third plateaux not being integer multiples of the singular event. Indeed, the difference in magnitude between successive higher order plateaux diminishes as the order increases, suggesting that the curvature of the tube is diminishing as the order, or radius, increases. We note that this behaviour should not necessarily appear in biological systems where, excepting certain organelles, the thickness of the membrane is limited to one bilayer. It is important to note that the distribution of plateau events does not depend on the tip radius; the results represented in Fig. 5 are collected data from eight different experiments. It is possible to obtain an estimate of the bending constant, κ, and of the radii of the withdrawn tubes from the basic model that follows. We take r_1, r_2 and r_3 as the radii of curvature of the membranes (taken at their midplane) comprising three concentric cylinders. We denote, d_0, as the half thickness of a bilayer and we will assume that the repeat distance, $d+2d_0$, retains the same value as for a fully hydrated L_β phase (6.38 nm [10]). The model can be expressed (Fig. 6):

$$r_1 = r_l + d_0$$

$$r_2 = r_l + 3d_0 + d$$

$$r_3 = r_l + 5d_0 + d \tag{2}$$

where, r_l, is the radius of the lumen and, d, is the water layer thickness. From Eq. (1) and our measurements of the plateau forces, we can write:

$$F_1 = \frac{\pi\kappa}{r_1} = 45.5 \pm 3.5 \text{ pN}$$

$$F_2 = F_1 \frac{\pi\kappa}{r_2} = 81.6 \pm 3.5 \text{ pN}$$

$$F_3 = F_2 \frac{\pi\kappa}{r_3} = 113 \pm 3.5 \text{ pN} \tag{3}$$

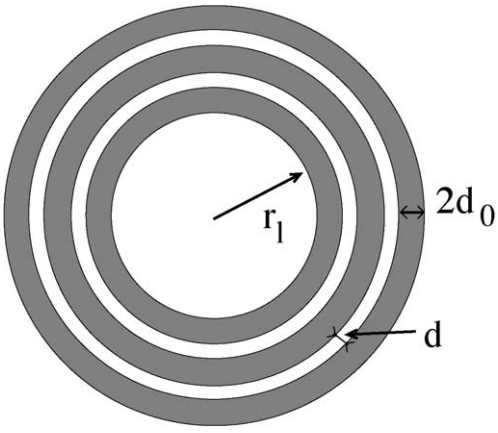

Fig. 6. Model for a three-layered tubule.

which leads to the following expression:

$$\frac{\pi\kappa}{F_i - F_{i-1}} = (r_l + d_0) + (i-1)(2d_0 + d) \tag{4}$$

with $F_0 = 0$. Our data are consistent with this latter expression and give a lumen radius of 26 ± 3 nm, from which we can deduce a bending rigidity constant of $100 \pm 10\ k_BT$. This value of the bending constant can be compared with recent optical measurements of DPPC bending constant in the gel state [19] (around 250 k_BT). Our estimation can also be compared to the result of the experiment of Hochmuth *et al.* [15,16]. where a tether was drawn out a human erythrocyte trapped in a micropipette. The radii of the tether ranged from 10 to 20 nm with an associated bending constant of 25 k_BT. But it should be pointed out here that the determination of a bending constant depends on the length scale and thus on the type (optical, mechanical) of measurement.

Our results show that the force required to draw cylindrical bilayers is only a small fraction of that needed for bilayer fusion. There is a considerable energy barrier for primary fusion, which may prevent each random collision of bacterial cells resulting in fusion. However, once the initial barrier is overcome, the formation of cylindrical tubes is energetically inexpensive and subsequent growth has a constant cost per unit length. The rupture of the connective tube may occur through the pulling of a hole defect into the tube, or simply by *using up* the available bilayer in that layer. A proposed scheme is shown in Fig. 7. Note that the relatively high energetic cost of exposing the hydrophobic inner membrane precludes the formation of a cylindrical micelle. It is clear that the SFA and AFM provide complementary information about membrane fusion and fission processes.

3.2. DMPC bilayers

In order to investigate the possible role of the lipid phase state on the plateau phenomenon, we repeated the above protocol with DMPC over the range 12 and 28 °C. Tran-

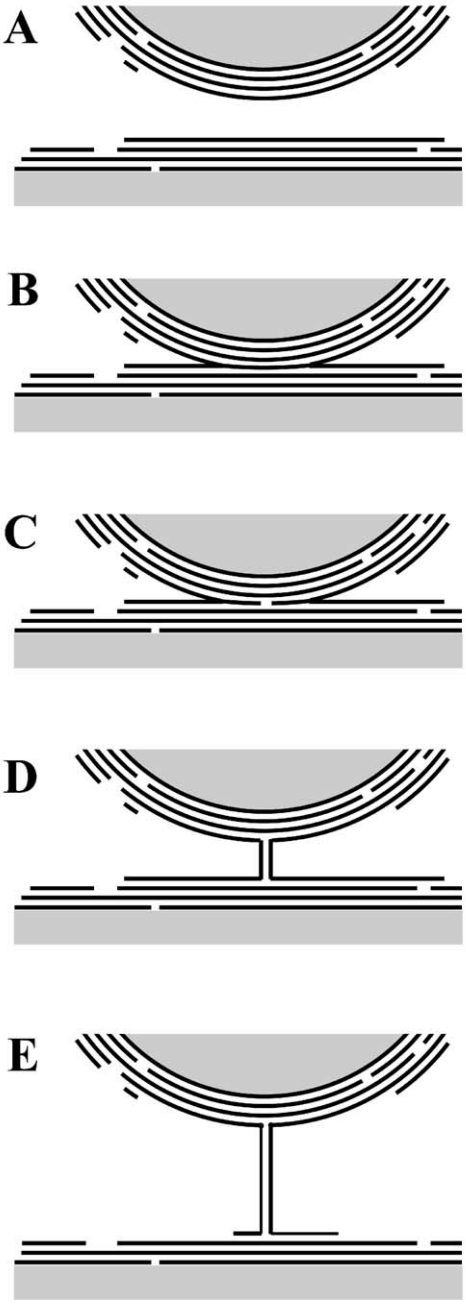

Fig. 7. A scheme showing the proposed formation of a vesicular tube upon the extension of fused phospholipid bilayers. The curved upper surface represents the AFM tip, approximately to scale. Each thick solid line corresponds to one bilayer. Steps A and B show the approach and fusion of opposed bilayers, after Horn [2]. Step B shows that on compression, a monolayer is excluded from each surface resulting in a single bilayer contact zone. The defective nature of this zone can lead to the formation of a hole, (step C). On retraction of the tip, (steps D and E), a tube is extended at the expense of the membrane which feeds into it. The relatively high energetic cost of exposing the hydrophobic inner membrane precludes the formation of a cylindrical micelle.

sition temperatures reported in multilamellar liposomes are 13.7 ± 2 °C for $L_{\beta'} \rightarrow P_{\beta}$, and 23.6 ± 1 °C for $P_{\beta} \rightarrow L_{\alpha}$ [5]. We did not observe any temperature-dependent features in the fission process. Indeed, AFM images have shown that the system was in the ripple state throughout all measurements. This was the case well into the region where L_{α} exists in bulk systems. We feel the observation reflects the difficulty for the water to permeate the supported bilayer stack. Note that the transition temperature typically decreases with water concentration [5]. Representative force curves, recorded at different temperatures, are presented in Fig. 8. Force plateaux are clearly visible but there are three distinctive features when compared with DPPC: (i) the average amplitude of the plateau forces is smaller by a factor of about 2, (ii) the average extension of the plateaux is much larger, by a factor of about 5, (iii) the plateau forces do not exhibit any pronounced quantization (Figs. 9 and 10). Nevertheless, one can distinguish a frequently observed force of about 20 pN (half that for DPPC bilayers). Assuming again that cylinders are withdrawn, we would obtain, an average bending constant value of about half the one of

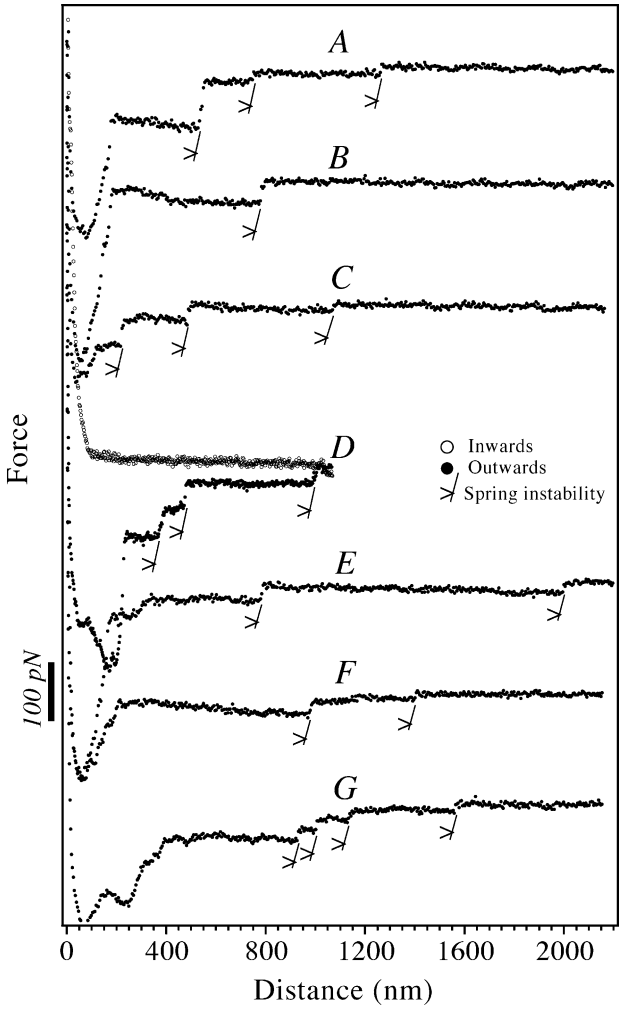

Fig. 8. DMPC: typical force curves recorded at different temperatures over the range 12–28 °C. One (B), two (E, F), three (A, C, D) or even four plateaux (G) can be distinguished on outwards curves. The inwards data are only shown on curve D.

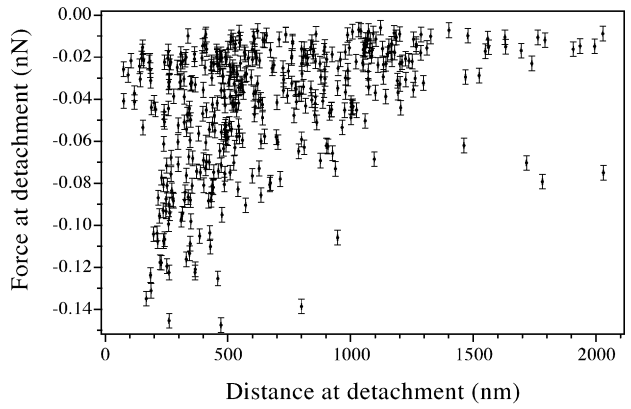

Fig. 9. DMPC: a scatter plot showing the points of plateau release for the data binned in Fig. 10. There is no sharp quantization as with DPPC bilayers (Fig. 4).

DPPC, *i.e.* $\simeq 50\ k_BT$. The study of Dimova *et al*. [20] has reported a variation of this bending rigidity constant for DMPC in the ripple phase from about 800 k_BT at 18 °C down to 10 k_BT at the transition towards the liquid crystalline phase L_α. DPPC, on the other hand, exhibits a variation from 250 k_BT down to 25 k_BT on increasing the temperature within the ripple phase domain [19].

In our model of (multi)tubule stretching, the membrane has to bend strongly at the tube–flat membrane junction. We may assume that this bending requires the melting of the membrane in order to enter the L_α phase. The ratio of the bending constants obtained by our estimation for DPPC and DMPC, might thus well reflect the ratio of the values at the melting temperatures [19,20]. The ripple phase of phospholipids has been recently described as a pre-transition phase where molecules can be in the gel (L_β) or in the liquid crystalline (L_α) state depending on their position in the corrugated structure [21]. This phase heterogeneity might be responsible for the poorer definition of the structures drawn by the AFM tip for DMPC. Nevertheless, we have no clear explanation for why DMPC permits larger extensions of the structures than does DPPC.

3.3. Swelling of lipid mixtures

A simple and efficient way to produce very large (giant) unilamellar vesicles has been invented by Angelova and Dimitrov [1] and consists of applying an alternating electrical field across a thin cell in which the walls have been coated with phospholipids. This method is very efficient, but its working remains quite mysterious. A first step in the understanding of the formation of vesicles under an electrical field is to the study of the swelling of phospholids films water in the absence of an applied electrical field. To this end, we applied a lipid mixture, known to spontaneously swell in water. We have used a liposome-forming kit purchased from Sigma (see Section 2). Again, a chloroform solution of this kit was simply evaporated on a freshly cleaved mica surface. Water was then added to the dried phospholipid layers just prior to engaging the AFM tip. The bilayers formed from the liposome kit are positively charged while the mica surface is negatively charged, thus ensuring strong adsorption. The bilayers are in a molten state at room temperature. Fig. 11a is characteristic of the swelling of the stack of bilayers deposited on the mica surface. *Blisters*,

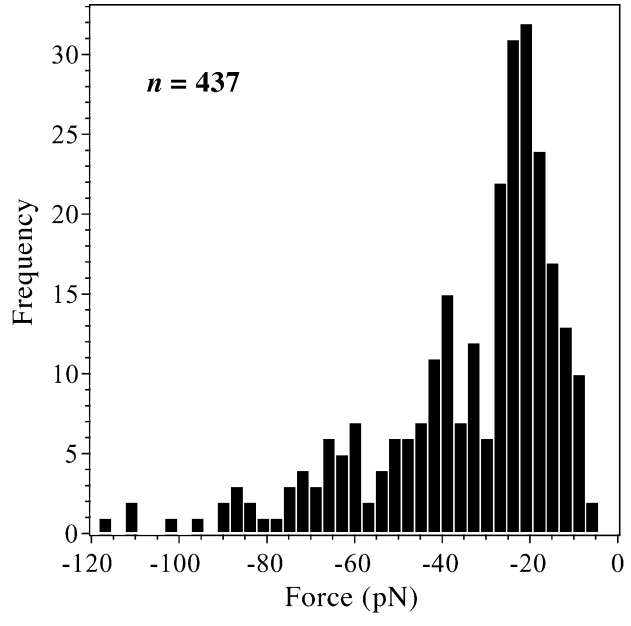

Fig. 10. DMPC: histogram of the force difference between plateaux on the *same* force curve during the *same* extension (437 events of plateau release).

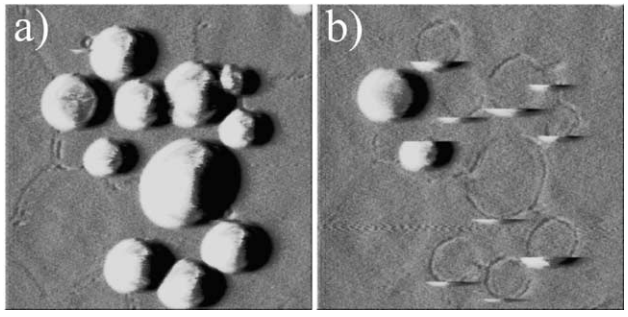

Fig. 11. AFM images ($886 \times 886\ nm^2$) of *blisters*. (a) The largest blister height is 24 ± 2 nm, while the other blisters have a height of about 13 ± 2 nm. All blisters exhibit a shoulder (see Fig. 12), which is 6.6 ± 1 nm above the base plane. This image was obtained by scanning approximately 100 nm from bilayer contact. This was achieved due to the repulsive electrostatic interaction between the surfaces [23]. (b) By decreasing the separation, the tip collides and bursts blisters above a certain height. These are revealed as *crescents* with a shallow groove where the blister once existed. These grooves are $\simeq 0.3$ nm deep and $\simeq 30$ nm wide. The only surviving blister in (b) consists only of the 6.6 nm shoulder discussed in the text. The image was scanned upwards and from left to right. The data shown is from deflection mapping. All height information has been taken from the corresponding height image (not shown).

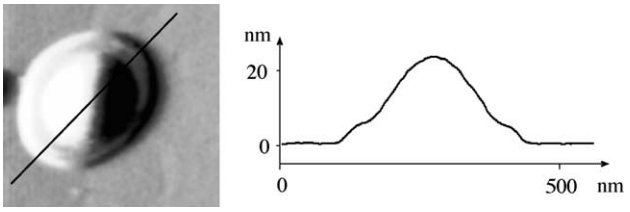

Fig. 12. Left: constant height view of a swollen blister. Right: height profile (along the line on the micrograph) showing the 6.6-nm-high, 50-nm-wide shoulder.

precursor structures of vesicles, are clearly visible. Fig. 11b shows that these structures can be easily destroyed when the contact imaging force is increased above a certain limit. Fig. 12 is an enlargement of a blister. There is a shoulder around each blister with a consistent height of 6.6 nm height. We believe that the bilayer in the shoulder region is still bound to the underlying stack of bilayers through van der Waals interactions while the bilayer defining the dome of the blister is unbound: here, repulsive Helfrich undulation forces dominate the attractive van der Waals forces [22].

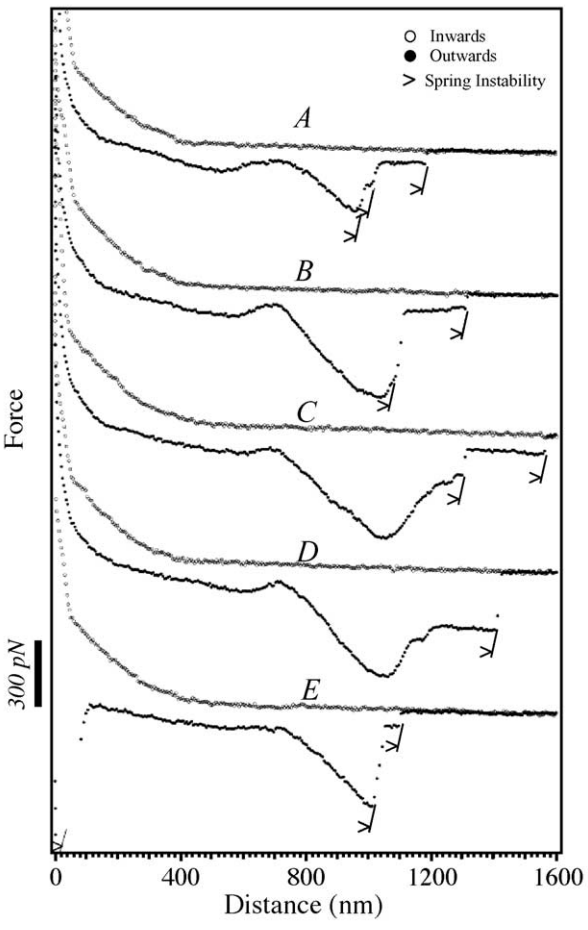

Fig. 13. Characteristic force curves obtained with the lipid mixture. All curves show on approach a first electrostatic repulsive part followed by a hard core type repulsion. On withdrawal, only (E) exhibits a first primary adhesion. See text for details.

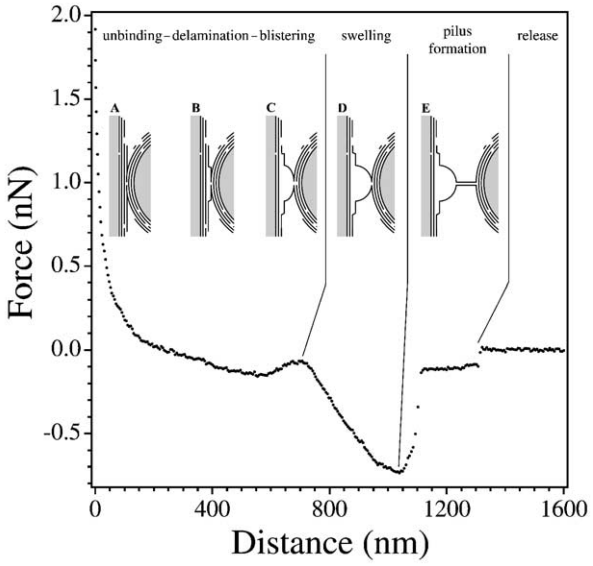

Fig. 14. Schematic scenario of the fission of a blister. (A) Initial fusion, (B, C) unbinding of the top-most bilayer and formation of the blister, (D) growth of the blister, (E) formation and entrainment of a tubule.

Finally, we report in Fig. 13 the characteristic forces experienced by an AFM tip. The first repulsive part on approach is simply due to the electrostatic double-layer interaction as the tip and mica are both covered with positive bilayers. The characteristic decay length of the repulsion of order 100–200 nm and is in good agreement with the expected value for water. A hard core type and hydration repulsion follows at shorter separation distances. The profile on separation of the fused surfaces presents a richer and puzzling structure and we can only hope to speculate on the mechanical details based on observations. A very tentative scenario is sketched in Fig. 14. At first, the force (attractive) decreases with distance and corresponds to the progressive reduction in fused area. This is followed by an unbinding process where the bilayer separation increases forming a shoulder, or flat-topped blister. Under continued extension, the flat-top pops up to form a curved blister, which through elastic deformation and lateral spread, grows to some limit. At some point, the material yields and a tubule is drawn from the blister itself. It is difficult to know how the bilayer components are distributed during this process.

4. Conclusion

We have reported in this paper a first study on the water swelling of phospholipids using the atomic force microscope. Some model scenarios require further investigations and have raised many questions. The possibility to form tubules from the fission of bilayers seems most promising,

and these results may have implications for the *initial* stages of bacterial conjugation. Much is known about the translocation of DNA during conjugation [24–32], however, much less is clear concerning the conjugative apparatus, or F-pilus [26,31]. Many studies suggest that cell to cell contact is necessary to induce pilus formation, and that in general, pili are approximately 8 nm in diameter with a central, 2-nm-wide hydrophilic lumen [31]. Although, the structural protein, F-pilin, is known to have a crucial role in the mature conjugative apparatus, the initiation and development of pili is still poorly understood. The role of other cell membrane components, such as lipids, in this apparatus has been largely ignored. Although cryo-transmission electron micrographs show no evidence of lipids in pili, there is some ambiguity concerning whether all the pilus components are preserved intact. Our model supports the established findings [24–32] and presents solutions to problems other models face. Since the protein, pilin, exists on both sides of the cell membrane, it may be incorporated into the tube as it is formed. Subsequent cross-linking of the pilin could result in a robust pilus. In proposing that cellular lipids are involved in the pilus, the main issues concerning DNA translocation can be addressed. Neither the hydrophobic region of the membrane nor the negatively charged surfaces pose a barrier for the passage of hydrophilic and negatively charged DNA, for the cells would be topologically connected via the structure described here.

Acknowledgements

The authors gratefully acknowledge helpful discussions with Stjepan Marcelja and Jan Hoh. JMdM would like to thank the Department of Applied Mathematics of the Research School of Physical Sciences and Engineering for supporting his stays in Canberra. TJS thanks the Australian Research Council for their support through a postdoctoral research fellowship.

References

[1] M.I. Angelova, D.S. Dimitrov, Faraday Discuss. Chem. Soc. 81 (1986) 303–311.
[2] R.G. Horn, Biochim. Biophys. Acta 778 (1984) 224–228.
[3] C.A. Helm, J.N. Israelachvili, P.M. McGuiggan, Science 240 (1989) 919–922.
[4] A. Tardieu, V. Luzzati, F.C. Reman, J. Mol. Biol. 75 (1977) 711–733.
[5] R. Koynova, M. Caffrey, Biochim. Biophys. Acta 1376 (1998) 91–145.
[6] J.Y. Wong, J. Majewski, M. Seitz, C.K. Park, J.N. Israelachvili, G.S. Smith, Biophys. J. 77 (1999) 1445–1457.
[7] J.Y. Wong, C.K. Park, M. Seitz, J.N. Israelachvili, Biophys. J. 77 (1999) 1458–1468.
[8] E. Sackmann, Science 271 (1996) 43–48.
[9] N. Maeda, T.J. Senden, Langmuir 16 (2000) 9282–9286.
[10] R.P. Rand, V.A. Parsegian, Biochim. Biophys. Acta 988 (1989) 351–376.
[11] R.E. Waugh, Biophys. J. 38 (1982) 19–27.
[12] R.E. Waugh, Biophys. J. 38 (1982) 29–37.
[13] R.E. Waugh, R.M. Hochmuth, Biophys. J. 52 (1987) 391–400.
[14] J. Song, R.E. Waugh, Biophys. J. 64 (1993) 1967–1970.
[15] R.M. Hochmuth, E.A. Evans, Biophys. J. 39 (1982) 71–81.
[16] R.M. Hochmuth, H.C. Wiles, E.A. Evans, J.T. McCown, Biophys. J. 39 (1982) 83–89.
[17] M. Schneider, J. Jenkins, W. Webb, Biophys. J. 45 (1984) 891–899.
[18] E. Evans, W. Rawicz, Phys. Rev. Lett. 64 (1990) 2094–2097.
[19] C.-H. Lee, W.-C. Lin, J. Wang, Phys. Rev. E 64 (2001) 020901 (R).
[20] R. Dimova, B. Pouligny, C. Dietrich, Biophys. J. 79 (2000) 340–356.
[21] T. Heimburg, Biophys. J. 78 (2000) 1154–1165.
[22] R. Lipowsky, S. Leibler, Phys. Rev. Lett. 56 (1986) 2541–2544.
[23] T.J. Senden, C.J. Drummond, P. Kékicheff, Langmuir 10 (1994) 358–362.
[24] C.M. Amabile-Cuevas, M.E. Chicure, Cell 70 (1992) 189–190.
[25] K.G. Anthony, W.A. Klimke, J. Manchak, L.S. Frost, J. Bacteriol. 181 (1999) 5149–5159.
[26] B. Dreiseikelmann, Microbiol. Rev. 58 (1994) 293–299.
[27] K.L. Fullner, J.C. Lara, E.W. Nester, Science 273 (1996) 1107–1109.
[28] J. Haase, E. Lanka, J. Bacteriol. 179 (1997) 5728–5735.
[29] M.T. Howard, W.C. Nelson, S.W. Matson, J. Biol. Chem. 270 (1995) 28381–28386.
[30] E.A. Sia, D.M. Kuehner, D.H. Figurski, J. Bacteriol. 178 (1996) 1457–1464.
[31] P.M. Silverman, Mol. Microbiol. 23 (1997) 423–429.
[32] N. Willetts, B. Wilkins, Microbiol. Rev. 48 (1984) 24–41.